IRIS AperTO

UNIVERSITÀ DEGLI STUDI DI TORINO

AperTO - Archivio Istituzionale Open Access dell'Università di Torino

Mobility of crocidolite asbestos in sandy porous media mimicking aquifer systems

This is a pre print version of the following article:

Original Citation:

Availability:

This version is available http://hdl.handle.net/2318/1930492 since 2023-09-06T15:07:12Z

Published version:

DOI:10.1016/j.jhazmat.2023.131998

Terms of use:

Open Access

Anyone can freely access the full text of works made available as "Open Access". Works made available under a Creative Commons license can be used according to the terms and conditions of said license. Use of all other works requires consent of the right holder (author or publisher) if not exempted from copyright protection by the applicable law.

(Article begins on next page)

07 May 2024

Mobility of crocidolite asbestos in sandy porous media mimicking aquifer systems

*Leonardo Magherini[1], Chiara Avataneo[2,3], Silvana Capella[2,3], Manuela Lasagna[2], Carlo Bianco[1], Elena Belluso[2,3,4], Domenico Antonio De Luca[2], Rajandrea Sethi[1,5]**

[1] Department of Environment, Land and Infrastructure Engineering (DIATI), Politecnico di Torino, Corso Duca degli Abruzzi 24, 10129 Turin, Italy
[2] Department of Earth Sciences, University of Turin, Via Valperga Caluso 35, 10125 Turin, Italy
[3] "G. Scansetti" Interdepartmental Center for Studies on Asbestos and Other Toxic Particulates, University of Turin, Via Pietro Giuria 7, 10125 Turin, Italy
[4] Geosciences and Earth Resources (IGG) of the National Research Council of Italy (CNR), Operational Unit of Turin, Via Valperga Caluso 35, 10125 Turin, Italy
[5] Clean Water Center (CWC), Politecnico di Torino, Corso Duca degli Abruzzi 24, 10129 Turin, Italy
** Corresponding author at: Department of Environment, Land and Infrastructure Engineering (DIATI), Politecnico di Torino, Corso Duca degli Abruzzi 24, 10129 Turin, Italy. E-mail address: rajandrea.sethi@polito.it*

Abstract

Asbestos is widely recognized as being a carcinogen when dispersed in air, but very little is known about its exposure pathways in water and its subsequent effects on human health. Several studies have proved asbestos presence in groundwater but failed to assess its mobility in aquifer systems. This paper aims to fill this gap by studying the transport of crocidolite, an amphibole asbestos, through sandy porous media mimicking different aquifer systems. To this purpose, two sets of column test were performed varying the crocidolite suspension concentration, the quartz sand grain size distribution, and the physicochemical water parameters (i.e., pH). The results proved that crocidolite is mobile in quartz sand due to the repulsive interactions between fibres and porous media. The concentration of fibres at the outlet of the column were found to decrease when decreasing the grain size distribution of the porous medium, with a bigger impact on highly concentrated suspensions. In particular, 5-to-10-µm-long fibres were able to flow through all the tested sands while fibres longer than 10 µm were mobile only through the coarser medium. These results confirm that groundwater migration should be considered a potential exposure pathway while implementing human health risk assessment.

Environmental implication

Asbestos is widely recognized as a human carcinogen when inhaled, but its adverse effects in water are still being disputed. Since waterborne asbestos can be ingested or inhaled due to nebulization or vaporization, a precise evaluation of its mobility in the aquifer system - one of the largest sources of freshwater for human consumption - is essential to perform an accurate human health risk assessment and estimate an exposure concentration level. Our laboratory study has confirmed crocidolite (an amphibole asbestos) mobility and transport in porous media, confirming that groundwater is a potential asbestos migration pathway.

Keywords

Asbestos transport, Fibre mobility, Crocidolite, Groundwater, Column test

1 Introduction

Asbestos is the commercial term that indicates a group of six naturally occurring silicate minerals with fibrous morphology. This group includes one serpentine phyllosilicate (chrysotile) and five amphiboles, which are chain silicates (tremolite asbestos, actinolite asbestos, anthophyllite asbestos, amosite, and crocidolite). In the past, these minerals have been widely employed for industrial applications due to their valuable technological properties, such as resistance to heat, fire, chemical and biological degradation. Nowadays their application has been drastically decreased, or even banned by several countries (IBAS, 2023), due to their adverse effects on human health. Indeed, the International Agency for Research on Cancer classifies asbestos as carcinogenic of the first group (IARC, 2012) and it is widely recognized as an air pollutant. For this reason, the European Union (EU) established an air concentration limit in the workplace for respirable fibres, i.e. fibres with length > 5 µm, width < 3 µm and aspect ratio (AR, length to width) > 3 (WHO, 1986), which are the ones considered to have carcinogenic effects when inhaled. The limit is 100 fibres per litre (f/L) (Directive 2009/148/EC) and is applied to the average air concentration measured during an 8 hour work shift. The same limit is also applied in the United States by the U.S. Occupational Safety and Health Administration (OSHA, 2021).

In the last decades, the attention of researchers and regulators shifted from occupational to environmental exposure scenarios. In particular, asbestos can be released by the erosion of Naturally Occurring Asbestos (NOA) or by mining and industrial activities (e.g. Mensi et al., 2015; Reid et al., 2007). An outdoor attention threshold of 1 f/L for ambient air was therefore proposed by the EU in the air quality guidelines to regulate asbestos exposure in non-occupational environments (WHO, 2000).

Up until recently, legislations on asbestos have however only focused on regulating its presence in air, neglecting to consider migration pathways and subsequent human exposure via water. This is partially due to the fact that the effects of waterborne asbestos ingestion on human health are still unclear and have only recently begun to be studied by the scientific community (Malinconico et al., 2022; Di Ciaula, 2017; Fortunato and Rushton, 2015).(WHO, 2021) The current literature identifies two main human exposure pathways for waterborne asbestos: (i) direct ingestion of asbestos containing water or beverages (Cunningham and Pontefract, 1971); (ii) inhalation of nebulised contaminated water droplets (e.g. Avataneo et al., 2022; Roccaro and Vagliasindi, 2018) or of resuspended fibres after polluted water vaporisation/evaporation. For the first scenario, the U.S. Environmental Protection Agency (US-EPA) established a maximum contaminant level in drinking water of $7 \cdot 10^6$ f/L for fibres longer than 10 µm (US-EPA, 2021) as a precautionary measure based on in vivo studies (NTP, 1985). Instead, the legislation regarding airborne asbestos and its limits could be applied to the second scenario, but it has been traditionally neglected, even if it can determine a significant inhalation exposure.

Besides drinking water, also freshwater resources should be monitored, in particular groundwater, which is one of the main sources of water for human consumption and anthropogenic activities. Indeed, groundwater is at the basis of many agricultural and industrial activities, as well as drinking water supply plants (e.g. Koumantakis et al., 2009). The presence of asbestos in groundwater has been documented by several studies, which found fibres in aquifers that are naturally rich in asbestos (Avataneo et al., 2021; Wei et al., 2013; Hayward, 1984; Oliver and Murr, 1977) or in areas where the mobilization of the fibres is further enhanced by human activities, e.g. in the proximity of mines and mine tailing deposits (Turci et al., 2016; Kashansky and Slyshkina, 2002; Buzio et al., 2000). More specifically, three studies have investigated asbestos occurrence in groundwater close to the former chrysotile

mine of Balangero, Italy (Avataneo et al., 2021; Turci et al., 2016; Buzio et al., 2000). Based on analyses by Scanning Electron Microscopy coupled with Energy Dispersive Spectroscopy (SEM-EDS), Buzio et al. (2000) detected an asbestos content of 1.00 ± 4.10 mg/L in groundwater and reported that the presence of fibres was reduced by a factor 10 at a distance of 5 km from the mine discharge. Similarly, Turci et al. (2016) monitored two wells in proximity of the former mine and detected over 10^6 f/L in the sampling point close to the mine southern tailings. Avataneo et al. (2021) instead reported a very variable asbestos content in wells or piezometers located in the alluvial plain close to the former asbestos mine of Balangero. Based on Transmission Electron Microscopy (TEM)-EDS, fibres up to 13 µm long were found in a sampling point with a concentration of $6.7 \cdot 10^6$ f/L (corresponding to 2 µg/L). Conversely, a study conducted on three drainage pits located next to a Russian asbestos deposit showed a very low asbestos concentration detected by means of Phase Contrast Optical Microscopy. The maximum concentration was $0.99 \cdot 10^5$ f/L with fibres longer than 5 µm ranging between 9.82% to 44.58% of the total (Kashansky and Slyshkina, 2002). Studies conducted in the U.S. in the '70 and '80 on samples collected from wells and springs and analysed by TEM-EDS showed the occurrence of asbestos in groundwater, mainly caused by the leaching of asbestos from the host rock formations. In particular, asbestos concentrations in the range $2 \cdot 10^7$-$2 \cdot 10^8$ f/L were found in California (Hayward, 1984), while values over $2 \cdot 10^9$ f/L (0.91 µg/L) were found along the Rio Grande Valley, New Mexico (Oliver and Murr, 1977). In the Dayao region, China, a thin layer of outcrop crocidolite ore is spread on an area of around 200 km^2, resulting in an average groundwater asbestos contamination of $8.6 \cdot 10^6$ f/L, detected by SEM-EDS analyses (Wei et al., 2013).(e.g., Hu and Hubble, 2007; Al-Adeeb and Matti, 1984)

The above-mentioned studies only focused on the presence of asbestos in groundwater, failing to consider the mobility and transport of fibres through the aquifer systems. Indeed, the mobility of asbestos in the subsurface has always been neglected or considered irrelevant in the literature (INAIL, 2022; Wallis et al., 2020; Paglietti et al., 2012). The contamination scenarios mentioned in previous studies can therefore imply relevant environmental and sanitary issues, especially if asbestos is able to migrate through porous media such as aquifer systems. An accurate study of asbestos mobility and transport is therefore needed to implement and integrate the knowledge of previous work to provide a comprehensive assessment of the health risks connected to migration via groundwater.

The well-established knowledge on particle transport in aquifer systems can be adapted to the case of asbestos. The colloidal transport in porous media is governed by advection, dispersion and by physical and physicochemical interactions with solid phase. Physical factors include the size and shape of the particles (Ting et al., 2021; Seymour et al., 2013; Pelley and Tufenkji, 2008), the characteristics of the porous medium and the flow conditions (Bradford et al., 2002). Thanks to their typical form factor (length >> width), fibres can flow through pores that are smaller than their length but bigger than their width. On the other side, the elongation of the particles associated with drag forces can lead to filtration due to mechanical and geometrical interactions with the porous medium (Seymour et al., 2013). These interactions are further increased by aggregation and tangling (Chequer et al., 2019; Wu et al., 2017). Water chemistry, especially ionic strength and pH, can strongly influence the transport of particles by modifying the intensity of the attractive/repulsive forces acting between the fibres and the porous medium (Pulido-Reyes et al., 2022; Beryani et al., 2020; Tian et al., 2012; Gronow, 1986).

The transport of particles is also affected by the electrostatic interactions between the particles and the porous media. Chrysotile, at neutral pH, is retained within the aquifer system due to the attractive electrostatic interaction between the positive surface charge of the fibres (Pollastri et al., 2014) and the net negative surface charge of the soil (Granetto et al., 2022). A recent study confirmed that bare chrysotile is not mobile in porous media but that, in presence of dissolved organic matter (DOM), its surface charge can be reverted thus allowing the subsurface transport (Mohanty et al., 2021). As opposed to serpentine phyllosilicate, amphiboles naturally exhibit a negative net surface charge in water at any pH (Pollastri et al., 2014). For this reason, these minerals are expected to be mobile in subsurface environments, due to the repulsive electrostatic interaction between the fibre and the negative surface of the porous medium.

The goal of this study is to verify if amphibole fibres, i.e. a naturally negatively charged asbestos, can be transported through saturated sandy aquifer systems without any surface modifier (or DOM). To this purpose, laboratory transport tests in sand-packed columns were performed using crocidolite as a representative amphibole asbestos. The tests were performed by varying the crocidolite concentration, the sand grain size distribution and the porewater composition with the aim to investigate: (i) to what extent crocidolite can be mobile in sandy porous media; (ii) how the size of fibres and pores affect the crocidolite mobility; (iii) if the groundwater physicochemical parameters influence the fibre transport.

2 Materials and methods

2.1 Asbestos suspensions

An asbestos suspension was prepared by adding crocidolite UICC (Union for International Cancer Control), a well characterised standard (Kohyama et al., 1996), to deionized water to obtain a 300 mg/L concentration. The crocidolite was dispersed in water applying sonication and stirring for about 25 minutes. The crocidolite suspension was characterised by a pH of 7.7 and a zeta potential of -30.2±0.4 mV in 0.01 M NaCl, measured by dynamic light scattering (DLS Zetasizer Nano Z, Malvern Instruments Ltd., U.K.). A 1 mM MOPS buffer (MOPS, 3-N-Morpholino propanesulfonic acid, Sigma-Aldrich) was added to stabilise the pH at 6-7.

Two batches were prepared:

- a high concentration suspension (hereafter referred to as HC) obtained by collecting the supernatant of the 300 mg/L crocidolite suspension after 5 hours settling;
- a low concentration suspension (hereafter referred to as LC) obtained by filtering the HC suspension through a coarse sand bed.

The batches were used to simulate two different scenarios: the asbestos transport near a concentrated contamination source using the HC batch, and the fibre fate at medium to long distance from the source thus using LC batch.

2.2 Porous media

Transport experiments were conducted in quartz sand (Dorsilit from Dorfner GmbH & Co., Germany). Three types of sand with different grain size distributions (Figure S1, Supplementary Information-SI), defined respectively coarse, medium, and fine, were tested. The measured values of d_{10}-d_{50}-d_{90} were 1.31-1.59-1.91 mm for coarse sand, 0.48-0.68-0.84 mm for medium sand and 0.26-0.49-0.58 mm for fine sand. Before use, the sand was thoroughly cleaned to remove any residual impurities and colloids. The cleaning procedure consisted of three cycles of washing and sonication with 100 mM NaOH, tap water and deionized water, respectively. After cleaning, the sand was dried with a laboratory hot plate.

Prior to packing the columns, a known quantity of dry sand was rehydrated in a 1 mM MOPS solution and degassed with a vacuum bell.

The zeta potential of each porous medium was measured in 0.01 M NaCl solution by DLS (Zetasizer Nano ZS90, Malvern Instruments Ltd., U.K.) and was equal to -46.8±1.0 mV, -49.1±2.6 mV and -52.5±0.6 mV, respectively for coarse, medium and fine sand.

The hydrodynamic parameters of the porous media, namely effective porosity and dispersivity, were determined by fitting a breakthrough curve (BC) of a conservative tracer (i.e. 10 mM NaCl in 1 mM MOPS). The estimated effective porosity was 47%, 43% and 39% for coarse, medium and fine sand, respectively. While the dispersivity was 0.47 mm for the coarse sand, 0.20 mm for the medium sand and 0.10 mm for the fine sand. The BCs and the parameters are reported in Figure S2 and Table S1 of SI, respectively.

2.3 Column test setup, sampling, and injection procedure

The experimental setup is outlined in Fig. 1. A column with internal diameter of 1.6 cm and total length of 11 cm was wet packed as follows: coarse sand was used to create a 0.5 cm drain at the column inlet and outlet; coarse, medium or fine sand, depending on the specific experiment conditions, were used to pack the 10 cm porous medium to be tested.

The crocidolite suspension, continuously stirred, was pumped into the saturated column with a peristaltic pump at a flow rate of 0.22±0.01 mL/min, corresponding to a Darcy velocity of 1.56±0.09 m/d. The injection schedule was applied for all the tests as described below.

(i) Preconditioning: 10 pore volumes (PV) of a 1 mM MOPS solution to equilibrate the sand column.
(ii) Injection: 6 PV of crocidolite suspension (HC or LC) to test the asbestos transport.
(iii) Flushing: 3 PV of a 1 mM MOPS solution to flush the system.
(iv) Release: 3 PV of a solution containing 1 mM MOPS and 100 mM NaOH (pH 13) to induce the detachment of the fraction of fibres that were reversibly deposited on the porous media during phase (ii).

During the experiments, the concentration of crocidolite suspension at the column outlet was measured online, via optical density measurements using a UV-vis spectrophotometer (Specord S600, Analytik Jena, Germany) equipped with a flow-through cell (Hellma, Germany). A linear relation between absorbance and crocidolite concentration was found at a wavelength of 285 nm (Figure S3-S4-S5, SI). Throughout the paper “C” will be used to refer to the absorbance of crocidolite concentration measured by the spectrophotometer for outlet liquid samples, whereas “C_0” to refer to the absorbance concentration at the inlet.

During the column tests “L” liquid samples (Fig. 1) were collected at the column outlet every 1 PV. At the end of each test, the column was dissected and porous medium “S” samples (Fig. 1) were collected every 1 centimetre to determine the mass of fibres filtered out by column. Both “L” and “S” sample types were then analysed by means of SEM-EDS.

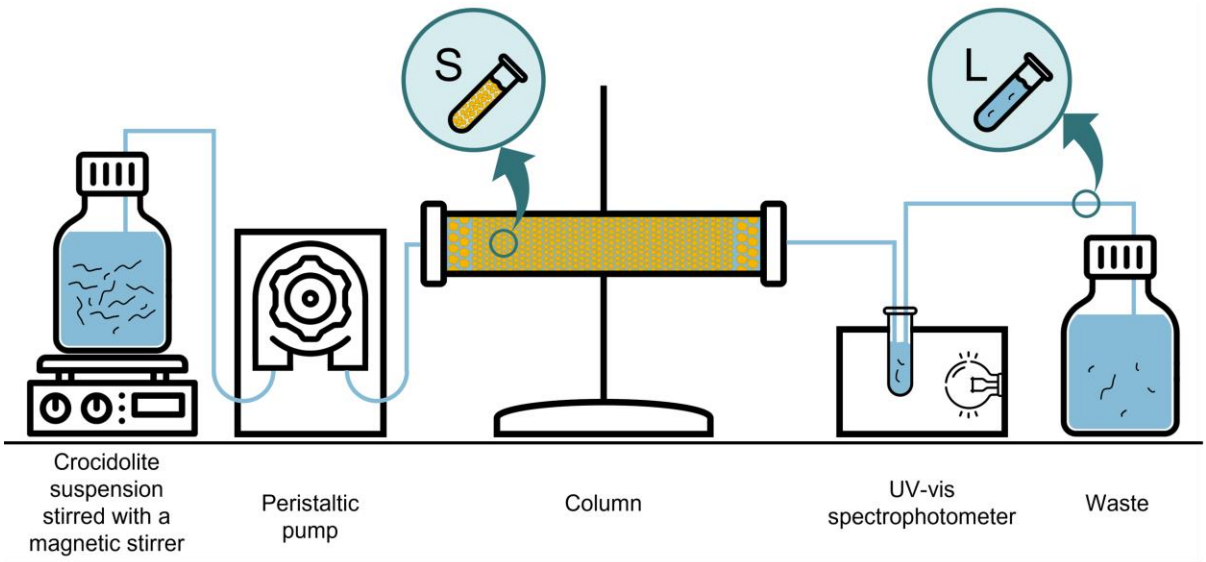

Fig. 1. Schematic rapresentation of the experimental setup used for crocidolite transport test; S and L represent, respectively, the solid and liquid sample location.

2.4 SEM-EDS analyses

Both liquid "L" and solid "S" samples were collected during each column test and analysed by means of SEM-EDS An aliquot (dependant on suspension turbidity) of the liquid samples was first filtered on a polycarbonate membrane (25 mm diameter, 0.1 µm porosity) using a vacuum filtration system. To prevent the sedimentation and agglomeration of fibres, samples were sonicated for 8 minutes before filtration. As regards solid samples, porous medium aliquots were resuspended in 10 mL deionized water and sonicated for 8 minutes to ensure the complete detachment of crocidolite from the sand fraction. A 0.1 mL aliquot of the supernatant was then filtered on polycarbonate membranes with the same procedure applied for liquid samples. All the filtering membranes were left to dry at room temperature, adequately covered to avoid any contaminations. Then, membranes were mounted on aluminium sample holders using graphite tape and coated by a conductive graphite layer.

All liquid and solid samples membranes were analysed by means of a JEOL JSM IT300LV SEM with W emitter, coupled with an EDS Oxford INCA Energy 200 X-act SDD thin window detector. 0.1 mm^2 of each membrane surface was scanned acquiring 0.003 mm^2 images with a resolution of 32 pixel/µm.

For liquid samples, crocidolite was counted regardless of length, width, or aspect ratio after verifying the chemical composition. Concentration in f/L was then calculated considering the volume of sample filtered through the porous membrane, following the method proposed by the Regional Agency for the Protection of the Environment of Piedmont (Italy) (ARPA-Piemonte, 2021). In addition to the fibre number, the SEM image analysis allowed to measure the length and width of the fibres and to estimate their volume and mass by approximating their shape to a cylinder and considering a crocidolite density of 3.37 g/cm^3 (US-EPA, 1983). The conversion of number concentration (f/L) into mass concentration (mg/L) was performed adapting an Italian guideline for massive samples investigations (DM 06/09/1994).

The quantitative analysis of liquid samples was performed only during the injection step (phase ii in section 2.3). A qualitative analysis was instead performed on the liquid samples collected during the release step (phase iv in section 2.3) to gain insights on the dimensional and morphological characteristics of the crocidolite released as a result of the pH variation of the flushing solution. As far as concern the "S" samples, SEM-EDS analyses were performed to

obtain qualitative data on the amount of crocidolite retained in different segments of the column.

Throughout the paper "F" will be used to refer to crocidolite concentration in number (f/L) measured by SEM-EDS, while "M" to crocidolite concentration in mass (mg/L). "F5" indicates the number concentration of fibres with AR > 3, width < 3 µm and length > 5 µm, "F10" indicates the number concentration of fibres with AR > 3, width < 3 µm and length ≥ 10 µm. Subscript "0" is added when the concentration refers to the injected suspensions.

3 Results and discussion

3.1 Characterisation of asbestos suspensions

The first batch, HC, shown in Fig. 2, was obtained by collecting the supernatant of the 300 mg/L crocidolite suspension after a 5 h settling. The suspension had an average concentration in number of $2.9 \cdot 10^{11}$ f/L (as shown in Table 1), which was evaluated by analysis of SEM images. The corresponding mass concentration of 92.9 mg/L was estimated as described in section 2.4. The mean value of F5 was $1.6 \cdot 10^{10}$ f/L (5.5% of the total) and the mean value of F10 was $2.8 \cdot 10^{9}$ f/L (1.0% of the total). The maximum AR value was 102, while the average value was 10. The HC size distributions are shown in Figure S6 (SI).

The second batch, LC, shown in Fig. 2, was obtained by filtering the HC suspension through a coarse sand bed using the setup described in section 2.3. The resulting suspension had a concentration in number of $9.9 \cdot 10^{10}$ f/L, shown in Table 2, corresponding to a mass concentration of 5.5 mg/L, similar to the mass concentration detected in aquifers in NOA-rich areas (Buzio et al., 2000). The F5 concentration was $1.1 \cdot 10^{9}$ f/L (1.1% of the total) and the F10 concentration was $2.1 \cdot 10^{8}$ f/L (0.2% of the total). The AR mean value was 8 with a maximum of 92. The LC size distributions are shown in Figure S6 (SI).

It must be noted that, despite the number concentration of fibres in the HC suspension is comparable to LC one ($2.9 \cdot 10^{11}$ f/L for the HC and $9.9 \cdot 10^{10}$ f/L for the LC), a substantial mass concentration difference between the two suspensions is observed (92.9 mg/L for the HC and 5.5 mg/L of the LC). This discrepancy between the number and mass concentration is justified by the different fibre size distribution in the two samples. In particular, the F5 value is higher in the HC suspension than in the LC one. These fibres contribute significantly to the total asbestos mass in the samples; indeed, the F5 amount is one order of magnitude higher in the HC suspension ($1.6 \cdot 10^{10}$ f/L) than in the LC one ($1.1 \cdot 10^{9}$ f/L). On the contrary, the LC suspension contains a high number of shorter fibres, which do not contribute significantly to the total asbestos mass in the samples.

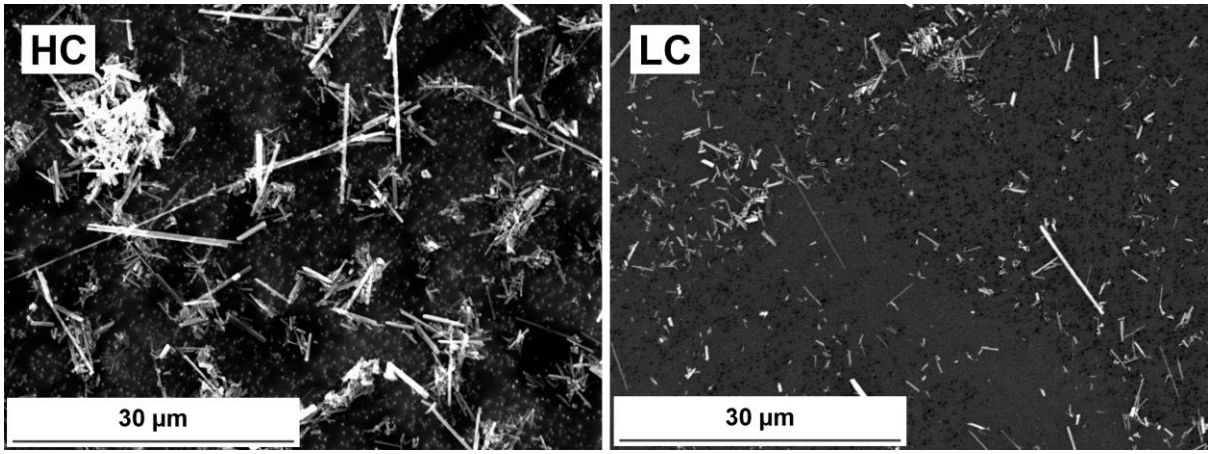

Fig. 2. SEM pictures of tested crocidolite suspensions. HC) high concentration suspension; LC) low concentration suspension.

3.2 Column transport tests

Two sets of transport tests, conducted by injecting crocidolite suspensions in 1D columns filled with sand material, were performed to probe the mobility of the fibres mimicking two realistic scenarios. The first set was conducted to simulate the mobility of a highly concentrated suspension (HC) in an aquifer system close to the source of contamination, the second to investigate the transport of a low concentrated suspension (LC) in a contaminated plume far from the release zone. The following sections describe the influence of asbestos size and concentration, and of the porous media granulometry, and of physicochemical parameters on the crocidolite mobility.

3.2.1 HC transport experiments

The first set of column tests was performed injecting the HC suspension through three types of quartz sand with different grain size distributions (coarse, medium and fine). The breakthrough curve (Fig. 3) of the experiment in coarse sand showed C/C_0 values greater than 20% during the whole injection step, with a maximum value of 30% observed at about 2 PV. Lower values, namely 2.2% and 0.3%, were respectively found for the medium and fine sand after 3 PV from the start of the injection. A higher retention of the crocidolite is observed when reducing the grain size distribution of the sand. This trend is also confirmed by the number concentration determined by SEM-EDS analyses (Table 1), which shows F values for the coarse, medium and fine sand equal to $5.7 \cdot 10^{10}$ f/L, $2.1 \cdot 10^{9}$ f/L, and $7.8 \cdot 10^{8}$ f/L respectively, for the liquid samples L2 collected after 3 PV at the outlet of the column. The corresponding M values, 3.69 mg/L for coarse, 0.22 mg/L for medium and 0.16 mg/L for fine sand, reflect the same tendency (Table 1). These results indicate that, despite a large amount of the injected asbestos is filtered out by the sandy media, a non-negligible fraction of the fibres is still mobile.

These results prove that crocidolite with a negatively charged surface can be transported, even in the absence of DOM, through negatively charged quartz sands. However, since only fibres longer than 5 µm (characterized by width < 3 µm and AR > 3) are considered dangerous to health if inhaled, it is of crucial importance to also assess the geometric characteristics of the fibres. As reported in Table 1, the average concentration of fibres longer than 5 µm ($F5_0$) in the injected HC suspension was equal to $1.6 \cdot 10^{10}$ f/L, the 17.5% of which consisted in fibres even longer than 10 µm ($F10_0$ equal to $2.8 \cdot 10^{9}$ f/L). All the outlet samples are characterized by a F5 count well above 10^{7} f/L and more specifically in the range $2.1 \cdot 10^{7}$-$5.3 \cdot 10^{8}$ f/L (Table 1). The concentrations of these samples are comparable or higher than the ones found in suspensions used by Avataneo et al. (2022) and by Roccaro and Vagliasindi (2018), who reported that waterborne values of $4.4 \cdot 10^{7}$ f/L and in the range $7.9 \cdot 10^{3}$-$2.5 \cdot 10^{4}$ f/L,

respectively, can cause an airborne contamination above the 1 f/L attention threshold (WHO, 2000), whether the water-to-air migration of fibres is triggered under specific conditions.

Fibres up to 18 µm were found in outlet samples of coarse and medium sand tests (see L_{max} in Table 1), while fibres up to 7 µm were measured in the fine sand test outlet. In particular, the 0.8% (coarse), 0.5% (medium) and 0.2% (fine) of $F5_0$ were recovered at the column outlet after 3 PV of suspension injection (L2, Fig. 4). Conversely, fibres longer than 10 µm were found only in sample L1 at the outlet of the coarse and medium sand columns. In these two samples the same F10 concentration value was found, $1.1 \cdot 10^8$ f/L, which is higher than the EPA maximum contaminant level for drinking water ($7 \cdot 10^6$ f/L for fibres longer than 10 µm). The results of the column tests performed at HC highlight that fibres longer than 10 µm barely migrate, while crocidolite with length between 5 and 10 µm might be substantially transported through sandy aquifers.

As far as concern transport mechanisms, the particles deposition in porous media is considered the result of both physical (i.e. mechanical filtration of thick particles in small pores) and physicochemical processes (i.e. particle attachment on the porous medium surface due to attractive particle-grain interaction forces). The first mechanism is typically assumed irreversible, meaning that no particle remobilization is expected upon a change of the pore water chemistry. As for attachment, instead, a variation of hydrochemical conditions (e.g. pH increase) may induce a detachment of the deposited particles due to the reduction of the attractive forces between the particles and the sand grains. In the case of crocidolite, physical filtration in small pores is expected to play a major role for the longer fibres. (Elimelech, 1995)(Bradford et al., 2002)(Lin et al., 2021) This is confirmed by SEM-EDS analysis of porous media sample collected at the first column centimetre for each tested sand (coarse, medium, and fine). All three samples (HC_S1_Coarse, HC_S1_Medium, HC_S1_Fine) presented a high number of fibres longer than 5 µm and even longer than 10 µm (Fig. 5). Moreover, visual inspection confirmed that the length of trapped fibres increases when decreasing the sand grain size distribution.

Another evidence confirming the occurrence of mechanical filtration is related to the evolution of the outlet concentration, which decreases over time once the filtered fibres start to clog the pores. This can be observed by the breakthrough curves reported in Fig. 3 where the absorbance ratio decreases from 30% to 22% for the coarse sand and from 2.5% to 1.5% for the medium sand. However, the decrease in absorbance is not evident for the fine sand, probably due to the low absorbance value detected. The increased filtration efficiency over time is also confirmed by the SEM-EDS analysis of the liquid samples collected at the column outlet, shown in Fig. 4. The graph shows a clear decrease over time (from sample L1 to sample L3) of the F5 values for all three quartz sands. In particular, the $F5/F5_0$ ratio decreases from 3.8% to 0.4% in coarse sand, from 2.7% to 0.2% in the medium sand, and from 0.18% to 0.16% in the fine one.

The release of reversibly attached fibres was induced by increasing the pH of the flushing water(Pulido-Reyes et al., 2022; Beryani et al., 2020; Tosco et al., 2009). As shown by the BCs in Fig. 3, a significant release peak is observed during the NaOH flushing for all three sand types. The peak height is inversely proportional to the sand grain size distribution, suggesting that physicochemical processes are more intense in the finer sand than in the coarser one due to the greater surface area of the porous medium in fine sand. A liquid sample was also collected during the release phase of the coarse sand column experiment and a SEM picture was acquired (Figure S7, SI). The image demonstrates the presence of fibres in the eluate, some of them with length of about 5 µm. This result indicates that, even

368 if initially retained by the porous medium, fibres may be remobilized if there is a change in
369 the aquifer hydrochemical conditions.

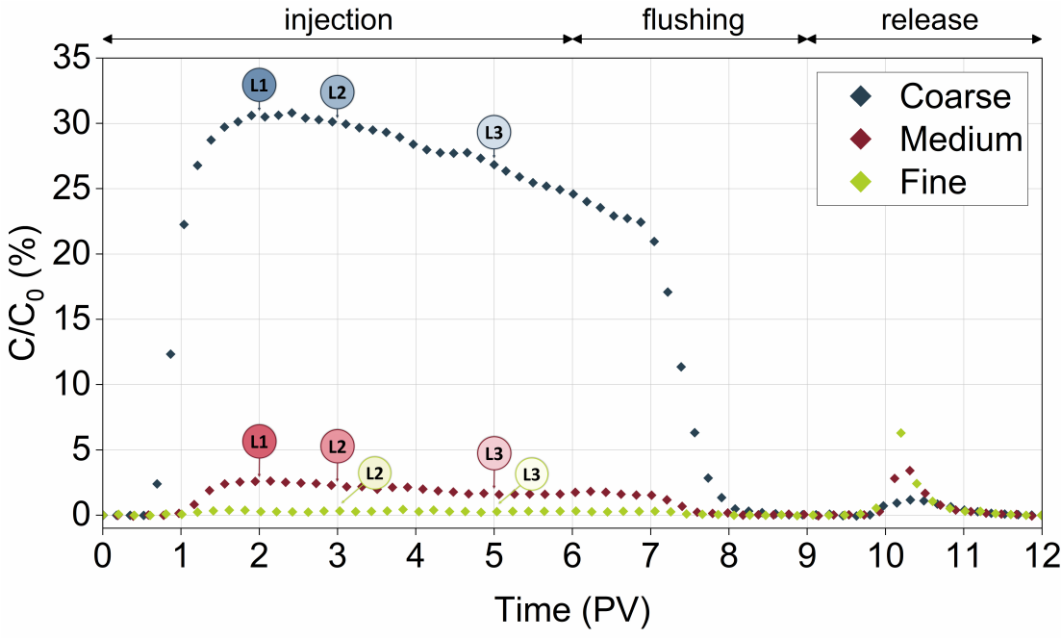

370

371 Fig. 3. Experimental breakthrough curves of normalized absorbance concentration of HC
372 crocidolite suspension during transport experiments performed in quartz sand with different
373 granulometry (coarse, medium, fine). Labels correspond to the liquid samples (L) collected at
374 the column outlet and analysed by SEM-EDS.

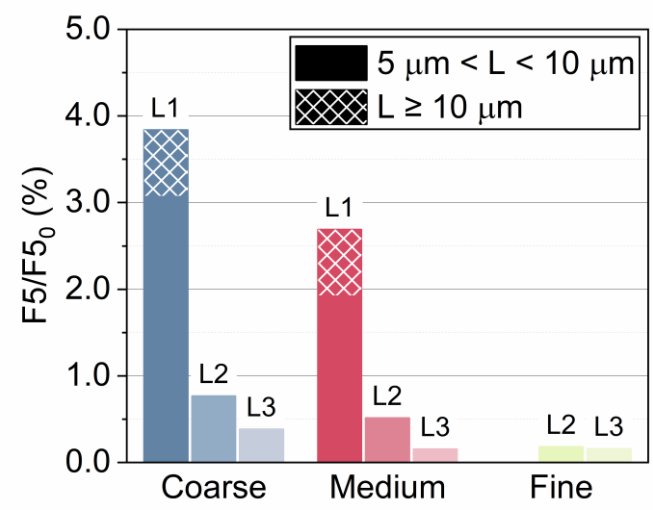

375

376 Fig. 4. Bar chart of concentration of fibres longer than 5 µm (F5) in liquid samples collected at
377 the column outlet (L1, L2, L3) as a percentage of concentration of fibres longer than 5 µm of
378 the HC suspension ($F5_0$) for the three tested sands (coarse, medium, fine); solid fill) the portion
379 of fibres longer than 5 µm and shorter than 10 µm; pattern fill) the portion of fibres longer than
380 (or equal to) 10 µm.

381

382

383

384

Table 1. F (f/L) and M (mg/L) concentrations of crocidolite in the inlet (HC) and in liquid samples collected at the column outlet (L1, L2, L3) during transport tests performed with the high concentration suspension (HC). F5, number concentration of fibres longer than 5 µm, and F10, number concentration of fibres longer than 10 µm values, are also reported. Dimension ranges (L=length, W=width) of detected fibres are reported for each sample. Additional details regarding quantitative results obtained on SEM-EDS analyses are reported in Table S2 (SI).

		F (f/L)	F5 (f/L)	F10 (f/L)	M (mg/L)	L_{min} (µm)	L_{max} (µm)	W_{min} (µm)	W_{max} (µm)
HC		2.9E+11	1.6E+10	2.8E+09	92.91	0.520	17.790	0.077	0.766
Coarse sand	L1	6.3E+10	5.3E+08	1.1E+08	3.81	0.292	18.138	0.044	0.554
	L2	5.7E+10	1.1E+08	-	3.69	0.311	6.205	0.062	0.560
	L3	3.7E+09	5.3E+07	-	0.56	0.330	7.343	0.083	0.466
Medium sand	L1	6.3E+09	3.7E+08	1.1E+08	2.25	0.517	18.248	0.069	0.532
	L2	2.1E+09	7.0E+07	-	0.22	0.436	6.151	0.056	0.348
	L3	2.1E+09	2.1E+07	-	0.22	0.404	6.468	0.075	0.405
Fine sand	L2	7.8E+08	3.0E+07	-	0.16	0.532	6.047	0.079	0.407
	L3	8.9E+08	2.6E+07	-	0.17	0.435	7.351	0.069	0.473

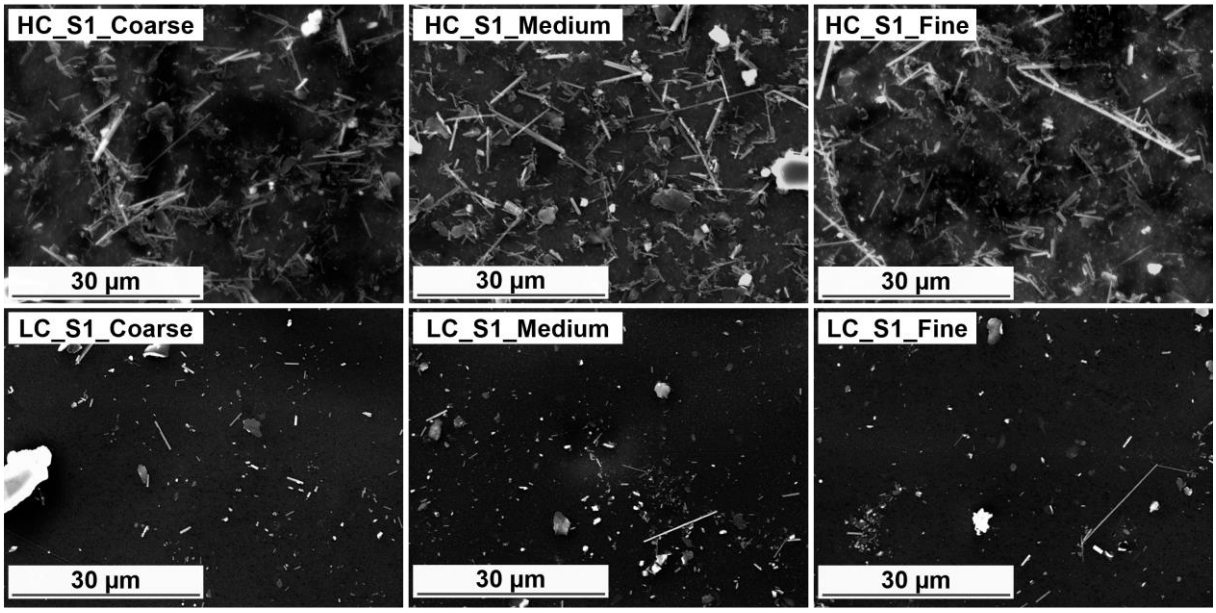

Fig. 5. SEM pictures of the porous media samples collected from the first column centimetre after the transport test with: HC suspension for coarse sand (HC_S1_Coarse), medium sand (HC_S1_Medium), fine sand (HC_L1_Fine); LC suspension for coarse sand (LC_S1_Coarse), medium sand (LC_S1_Medium), fine sand (LC_S1_Fine).

3.2.2 LC transport experiments

The second set of column tests was carried out injecting the LC suspension through the three porous media. The resulting normalized absorbance curves are shown in Fig. 6. Similarly to what observed for HC suspension, the BCs show an increase of the crocidolite retention when reducing the grain size distribution of the sand. However, overall, the crocidolite low

concentrated suspension shows a much higher mobility than the one observed during the HC experiments. The mobility increase is particularly pronounced for tests performed in the medium and fine sand, where the maximum value of C/C_0 increases from 1.1% (HC) to 18.4% (LC) for medium sand and from 0.5% (HC) to 9.7% (LC) for fine sand. The higher mobility of the LC suspension is probably due to the lower $F5_0$ value compared to HC one, in terms of both absolute number ($1.1 \cdot 10^9$ f/L for LC and $1.6 \cdot 10^{10}$ f/L for HC) and percentage on total (1.1% for LC and 5.5% for HC). The lower content of long fibres reduces the probability of porous medium clogging, which would have resulted in an increase of the filtration efficiency over time. This is confirmed by the shape of the BCs in Fig. 6 that, differently from what observed during the HC experiments, remain relatively constant during all the injection phases.

From the results of the SEM-EDS analysis, F5 values range between $1.1 \cdot 10^7$ and $1.5 \cdot 10^8$ f/L for the outlet liquid samples (Table 2), which are of the same order of magnitude as the HC tests. Interestingly, due to a lower porous media clogging, a F10 amount higher than the EPA threshold for drinking water was found in the L1 and L3 samples of the coarse sand (Table 2). The L2 liquid sample of the coarse sand test has a concentration of fibres longer than 5 µm abnormally lower than L1 and L3. This difference can be occurred due to an incorrect sampling or sample preparation. Looking at the normalized F5 value over time (Fig. 7) a net decreasing trend was not observed for the LC tests, in contrast with what observed for HC set in Fig. 4. This is a further evidence of a minor porous media clogging.

As for the HC experiments, a high pH flushing was performed at the end of the test to discriminate between reversible and irreversible fibre deposition. Despite the smaller amount of fibre retained in the column during the injection phase (i.e. higher BCs), the release peaks for the LC set result to be higher than for the HC tests. The absorbance peak varies from 18.0% to 68.8% for the tests performed with the LC suspension and from 1.2% to 6.3% for the HC one. This result suggests that asbestos transport may be influenced not only by mechanical filtration, but also by physicochemical reversible processes.

The SEM images of the porous media portions sampled from the first centimetre of each column (LC_S1_Coarse, LC_S1_Medium, LC_S1_Fine in Fig. 5) revealed the presence of fibres in all the samples. More specifically, they showed the presence of fibres longer than 5 µm and 10 µm, but in a smaller amount compared to the HC samples. This is further evidence that clogging is lower for LC suspension compared to HC, due to the lower number of fibres longer than 5 µm trapped in the sand. Moreover, being reversible processes higher for LC suspension, most of the shorter fibres were flushed during the NaOH release phase and therefore are not visible in Fig. 5. The SEM pictures of the liquid samples collected during the release phase (Figure S8, SI) show the presence of crocidolite with length up to 5 µm, particularly in medium and fine sand tests.

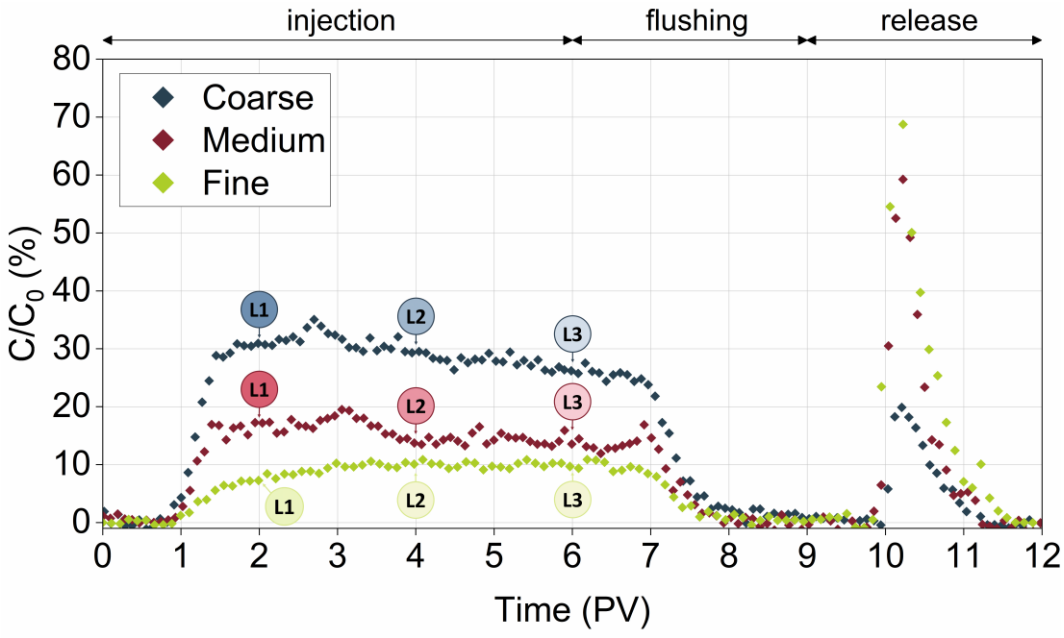

Fig. 6. Experimental breakthrough curves of normalized absorbance concentration of LC crocidolite suspension during transport experiments performed in quartz sand with different granulometry (coarse, medium, fine). Labels correspond to the liquid samples (L) collected at the column outlet and analysed by SEM-EDS.

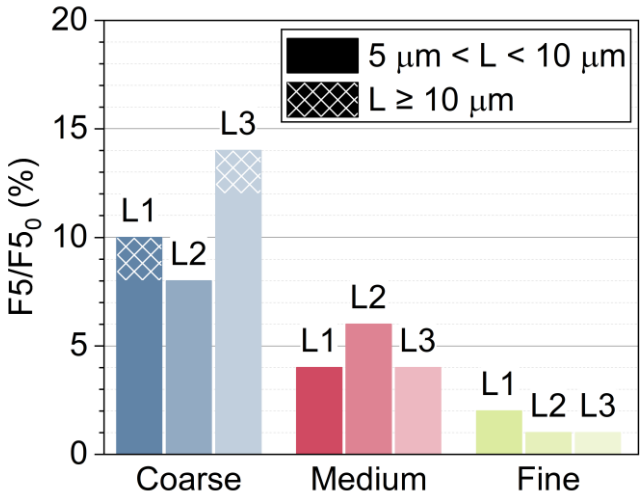

Fig. 7. Bar chart of concentration of fibres longer than 5 µm (F5) in liquid samples collected at the column outlet (L1, L2, L3) as a percentage of concentration of fibres longer than 5 µm of the LC suspension ($F5_0$) for the three tested sands (coarse, medium, fine); solid fill) the portion of fibres longer than 5 µm and shorter than 10 µm; pattern fill) the portion of fibres longer than (or equal to) 10 µm.

Table 2. F (f/L) and M (mg/L) concentrations of crocidolite in the inlet (LC) and in liquid samples collected at the column outlet (L1, L2, L3) during transport tests performed with the low concentration suspension (LC). F5, number concentration of fibres longer than 5 µm, and F10, number concentration of fibres longer than 10 µm values, are also reported. Dimension ranges (L=length, W=width) of detected fibres are reported for each sample. Additional details regarding quantitative results obtained on SEM-EDS analyses are reported in Table S3 (SI).

		F (f/L)	F5 (f/L)	F10 (f/L)	M (mg/L)	L_{min} (µm)	L_{max} (µm)	W_{min} (µm)	W_{max} (µm)
LC		9.9E+10	1.1E+09	2.1E+08	5.49	0.191	13.223	0.049	0.404
Coarse sand	L1	4.3E+09	1.1E+08	2.1E+07	1.14	0.435	11.830	0.104	0.528
	L2	5.8E+09	2.1E+07	-	0.93	0.354	5.044	0.070	0.551
	L3	6.5E+09	1.5E+08	2.1E+07	1.18	0.317	14.530	0.070	0.762
Medium sand	L1	5.4E+09	4.2E+07	-	0.43	0.243	8.821	0.070	0.379
	L2	3.8E+09	6.3E+07	-	0.39	0.267	9.189	0.066	0.423
	L3	2.3E+09	4.2E+07	-	0.28	0.386	6.683	0.088	0.325
Fine sand	L1	3.7E+09	2.1E+07	-	0.75	0.311	5.144	0.062	0.543
	L2	2.8E+09	1.1E+07	-	0.38	0.352	5.256	0.063	0.517
	L3	1.7E+09	1.1E+07	-	0.19	0.320	5.532	0.072	0.418

4 Conclusion

This study investigated the transport mechanism of waterborne crocidolite in saturated porous media mimicking sandy aquifers. Crocidolite was selected to represent amphibole asbestos behaviour, which exhibits negative net surface charge in water at any pH. Although asbestos mobility in subsoil has been generally neglected (or considered negligible), the results here presented show that bare crocidolite can be mobile in negatively charged porous media such as quartz sand aquifers.

Our results show that highly concentrated crocidolite suspensions generally determine lower breakthrough concentrations at the outlet of the columns due to the clogging of the porous medium which is induced mainly by the mechanical filtration of the longer fraction of the fibres. The decrease of the grain size distribution of the porous medium determines a strong decrease of the output concentrations further confirming the important role of mechanical filtration. On the contrary the injection of low concentration suspensions corresponds to a higher fibre recovery (if normalized to inlet concentration). Under these conditions, the decrease of the grain size of the porous media determines a less pronounced decrease in outlet concentrations. The transport is thus less influenced by the mechanical filtration (due to the reduced number of long fibres) but it is still dependent on the physicochemical interactions occurring under unfavourable deposition conditions (since the fibres and collectors are characterized by the same surface charge).

By characterizing the fibre suspensions sampled from the column outlet, we demonstrated that the medium and fine sandy media can retain most of the fibres longer than 10 µm, while 5-to-10-µm-long fibres can easily flow through. These results, obtained under specific laboratory conditions, might suggest that groundwater extracted downstream a contamination source is potentially safe to drink, but precautions should be taken to avoid water vaporization or fibre volatilization. In coarser aquifer systems also fibres longer than 10 µm can migrate

downwards a source of contamination determining a potential hazard for direct oral intake of contaminated groundwater.

In addition, our results indicate that a change in the water physicochemical parameters, e.g. a pH increase, can remobilize fibres primarily attached to the porous media, proving that waters considered safe to use can become potentially harmful after natural or human induced events that cause alterations of the groundwater geochemistry.

This study indicates that groundwater migration is a possible exposure pathway that should be included in human health risk assessment evaluations and that further studies have to be conducted to elucidate the risk induced by exposure to asbestos contaminated drinking water.

Acknowledgements

The authors gratefully acknowledge the contribution of Dr. Sofia Credaro, who assisted in the language editing of the manuscript.

References

Al-Adeeb, A.M., Matti, M.A., 1984. Leaching corrosion of asbestos cement pipes. International Journal of Cement Composites and Lightweight Concrete. https://doi.org/10.1016/0262-5075(84)90018-6

ARPA - Agenzia Regionale per la Protezione Ambientale del Piemonte, 2021. Asbestos in water by Scanning Electron Microscopy (Amianto in acqua in Microscopia Elettronica a Scansione). U.RP.M842, rev.05.

Avataneo, C., Belluso, E., Capella, S., Cocca, D., Lasagna, M., Pigozzi, G., De Luca, D.A., 2021. Groundwater asbestos pollution from naturally occurring asbestos (NOA): a preliminary study on the Lanzo valleys and Balangero plain area, NW Italy. Italian journal of engineering geology and environment 5–19. https://doi.org/10.4408/IJEGE.2021-01.S-01

Avataneo, C., Petriglieri, J.R., Capella, S., Tomatis, M., Luiso, M., Marangoni, G., Lazzari, E., Tinazzi, S., Lasagna, M., De Luca, D.A., Bergamini, M., Belluso, E., Turci, F., 2022. Chrysotile asbestos migration in air from contaminated water: An experimental simulation. Journal of Hazardous Materials. https://doi.org/10.1016/j.jhazmat.2021.127528

Beryani, A., Alavi Moghaddam, M.R., Tosco, T., Bianco, C., Hosseini, S.M., Kowsari, E., Sethi, R., 2020. Key factors affecting graphene oxide transport in saturated porous media. Science of the Total Environment 698. https://doi.org/10.1016/j.scitotenv.2019.134224

Bradford, S.A., Yates, S.R., Bettahar, M., Simunek, J., 2002. Physical factors affecting the transport and fate of colloids in saturated porous media. Water Resources Research 38, 63-1-63–12. https://doi.org/10.1029/2002WR001340

Buzio, S., Pesando, G., Zuppi, G.M., 2000. Hydrogeological study on the presence of asbestos fibres in water of northern Italy. Water Research 34, 1817–1822. https://doi.org/10.1016/S0043-1354(99)00336-X

Chequer, L., Bedrikovetsky, P., Carageorgos, T., Badalyan, A., Gitis, V., 2019. Mobilization of Attached Clustered Colloids in Porous Media. Water Resources Research 55, 5696–5714. https://doi.org/10.1029/2018WR024504

Cunningham, H.M., Pontefract, R., 1971. Asbestos fibres in beverages and drinking water. Nature 232, 332–333. https://doi.org/10.1038/232332a0

Di Ciaula, A., 2017. Asbestos ingestion and gastrointestinal cancer: a possible underestimated hazard. Expert Rev Gastroenterol Hepatol 11, 419–425. https://doi.org/10.1080/17474124.2017.1300528

Directive 2009/148/EC of the European Parliament and of the Council of 30 November 2009 on the protection of workers from the risks related to exposure to asbestos at work (Codified version) (Text with EEA relevance), 2009, OJ L.

DM 06/06/1994. Regulations and technical methods relating to the cessation of the use of asbestos (Normative e metodologie tecniche di applicazione dell'art. 6, comma 3, e dell'art. 12, comma 2, della legge 27 marzo 1992, n. 257, relativa alla cessazione dell'impiego dell'amianto).

Elimelech, M., 1995. Particle Deposition and Aggregation: Measurement, Modelling, and Simulation. Elsevier Science & Technology Books.

Fortunato, L., Rushton, L., 2015. Stomach cancer and occupational exposure to asbestos: A meta-analysis of occupational cohort studies. British Journal of Cancer 112, 1805–1815. https://doi.org/10.1038/bjc.2014.599

Granetto, M., Serpella, L., Fogliatto, S., Re, L., Bianco, C., Vidotto, F., Tosco, T., 2022. Natural clay and biopolymer-based nanopesticides to control the environmental spread

548 of a soluble herbicide. Science of The Total Environment 806, 151199.
549 https://doi.org/10.1016/j.scitotenv.2021.151199
550 Gronow, J.R., 1986. Mechanisms of particle movement in porous media. Clay Minerals 21,
551 753–767. https://doi.org/10.1180/claymin.1986.021.4.18
552 Hayward, S.B., 1984. Field Monitoring of Chrysotile Asbestos in California Waters. Journal
553 AWWA 76, 66–73. https://doi.org/10.1002/j.1551-8833.1984.tb05301.x
554 Hu, Y., Hubble, D.W., 2007. Factors contributing to the failure of asbestos cement water mains.
555 Can. J. Civ. Eng. 34, 608–621. https://doi.org/10.1139/l06-162
556 IARC Working Group on the Evaluation of Carcinogenic Risks to Humans, 2012. Arsenic,
557 metals, fibres, and dusts. IARC Monogr Eval Carcinog Risks Hum 100, 11–465.
558 IBAS - International Ban Asbestos Secretariat. Current Asbestos Bans. URL
559 http://ibasecretariat.org/alpha_ban_list.php (last accessed 30/01/2023).
560 INAIL - Istituto nazionale Assicurazione Infortuni sul Lavoro, 2022. Safe management of soils
561 contaminated by asbestos of anthropic origin (Gestione in sicurezza di suoli
562 contaminati da amianto di origine antropica).
563 Kashansky, S.V., Slyshkina, T.V., 2002. Asbestos in water sources of the Bazhenovskoye
564 chrysotile asbestos deposit. Int J Occup Med Environ Health 15, 65–68.
565 https://pubmed.ncbi.nlm.nih.gov/12038867/
566 Kohyama, N., Shinohara, Y., Suzuki, Y., 1996. Mineral phases and some reexamined
567 characteristics of the International Union Against Cancer standard asbestos samples.
568 Am J Ind Med 30, 515–528. https://doi.org/10.1002/(SICI)1097-
569 0274(199611)30:5<515::AID-AJIM1>3.0.CO;2-S
570 Koumantakis, E., Kalliopi, A., Dimitrios, K., Gidarakos, E., 2009. Asbestos pollution in an
571 inactive mine: Determination of asbestos fibers in the deposit tailings and water. Journal
572 of Hazardous Materials 167, 1080–1088.
573 https://doi.org/10.1016/j.jhazmat.2009.01.102
574 Lin, D., Hu, L., Bradford, S.A., Zhang, X., Lo, I.M.C., 2021. Pore-network modeling of colloid
575 transport and retention considering surface deposition, hydrodynamic bridging, and
576 straining. Journal of Hydrology 603, 127020.
577 https://doi.org/10.1016/j.jhydrol.2021.127020
578 Malinconico, S., Paglietti, F., Serranti, S., Bonifazi, G., Lonigro, I., 2022. Asbestos in soil and
579 water: A review of analytical techniques and methods. Journal of Hazardous Materials
580 436, 129083. https://doi.org/10.1016/j.jhazmat.2022.129083
581 Mensi, C., Riboldi, L., De Matteis, S., Bertazzi, P.A., Consonni, D., 2015. Impact of an
582 asbestos cement factory on mesothelioma incidence: global assessment of effects of
583 occupational, familial, and environmental exposure. Environ Int 74, 191–199.
584 https://doi.org/10.1016/j.envint.2014.10.016
585 Mohanty, S.K., Salamatipour, A., Willenbring, J.K., 2021. Mobility of asbestos fibers below
586 ground is enhanced by dissolved organic matter from soil amendments. Journal of
587 Hazardous Materials Letters 2, 100015. https://doi.org/10.1016/j.hazl.2021.100015
588 NTP - National Toxicology Program, 1985. NTP Toxicology and Carcinogenesis Studies of
589 Chrysotile Asbestos (CAS No. 12001-29-5) in F344/N Rats (Feed Studies). Natl
590 Toxicol Program Tech Rep Ser 295, 1–390.
591 Oliver, T., Murr, L. e., 1977. An Electron Microscope Study of Asbestiform Fiber
592 Concentrations in Rio Grande Valley Water Supplies. Journal AWWA 69, 428–431.
593 https://doi.org/10.1002/j.1551-8833.1977.tb06784.x
594 OSHA - Occupational Safety and Health Standards, 2021. 29 CFR 1910.1001.
595 Paglietti, F., Malinconico, S., Molfetta, V.D., Bellagamba, S., Damiani, F., Gennari, F., De
596 Simone, P., Sallusti, F., Giangrasso, M., 2012. Asbestos Risk: From Raw Material to
597 Waste Management: The Italian Experience. Critical Reviews in Environmental

598 Science and Technology 42, 1781–1861.
599 https://doi.org/10.1080/10643389.2011.569875
600 Pelley, A.J., Tufenkji, N., 2008. Effect of particle size and natural organic matter on the
601 migration of nano- and microscale latex particles in saturated porous media. Journal of
602 Colloid and Interface Science 321, 74–83. https://doi.org/10.1016/j.jcis.2008.01.046
603 Pollastri, S., Gualtieri, A.F., Gualtieri, M.L., Hanuskova, M., Cavallo, A., Gaudino, G., 2014.
604 The zeta potential of mineral fibres. Journal of Hazardous Materials 276, 469–479.
605 https://doi.org/10.1016/j.jhazmat.2014.05.060
606 Pulido-Reyes, G., Magherini, L., Bianco, C., Sethi, R., von Gunten, U., Kaegi, R., Mitrano,
607 D.M., 2022. Nanoplastics removal during drinking water treatment: Laboratory- and
608 pilot-scale experiments and modeling. Journal of Hazardous Materials 436, 129011.
609 https://doi.org/10.1016/j.jhazmat.2022.129011
610 Reid, A., Berry, G., de Klerk, N., Hansen, J., Heyworth, J., Ambrosini, G., Fritschi, L., Olsen,
611 N., Merler, E., Musk, A.W. (Bill), 2007. Age and Sex Differences in Malignant
612 Mesothelioma After Residential Exposure to Blue Asbestos (Crocidolite). Chest 131,
613 376–382. https://doi.org/10.1378/chest.06-1690
614 Roccaro, P., Vagliasindi, F.G.A., 2018. Indoor release of asbestiform fibers from naturally
615 contaminated water and related health risk. Chemosphere.
616 https://doi.org/10.1016/j.chemosphere.2018.03.040
617 Seymour, M.B., Chen, G., Su, C., Li, Y., 2013. Transport and Retention of Colloids in Porous
618 Media: Does Shape Really Matter? Environ. Sci. Technol. 47, 8391–8398.
619 https://doi.org/10.1021/es4016124
620 Tian, Y., Gao, B., Wang, Y., Morales, V.L., Carpena, R.M., Huang, Q., Yang, L., 2012.
621 Deposition and transport of functionalized carbon nanotubes in water-saturated sand
622 columns. Journal of Hazardous Materials 213–214, 265–272.
623 https://doi.org/10.1016/j.jhazmat.2012.01.088
624 Ting, H.Z., Bedrikovetsky, P., Tian, Z.F., Carageorgos, T., 2021. Impact of shape on particle
625 detachment in linear shear flows. Chemical Engineering Science 241, 116658.
626 https://doi.org/10.1016/j.ces.2021.116658
627 Tosco, T., Tiraferri, A., Sethi, R., 2009. Ionic Strength Dependent Transport of Microparticles
628 in Saturated Porous Media: Modeling Mobilization and Immobilization Phenomena
629 under Transient Chemical Conditions. Environ. Sci. Technol. 43, 4425–4431.
630 https://doi.org/10.1021/es900245d
631 Turci, F., Favero-Longo, S.E., Gazzano, C., Tomatis, M., Gentile-Garofalo, L., Bergamini, M.,
632 2016. Assessment of asbestos exposure during a simulated agricultural activity in the
633 proximity of the former asbestos mine of Balangero, Italy. Journal of Hazardous
634 Materials 308, 321–327. https://doi.org/10.1016/j.jhazmat.2016.01.056
635 US-EPA - United States Environmental Protection Agency, 2021. 40 CFR 141.62.
636 US-EPA - United States Environmental Protection Agency, 1983. Analytical method for
637 determination of asbestos fibers in water.
638 Wallis, S.L., Emmett, E.A., Hardy, R., Casper, B.B., Blanchon, D.J., Testa, J.R., Menges,
639 C.W., Gonneau, C., Jerolmack, D.J., Seiphoori, A., Steinhorn, G., Berry, T.-A., 2020.
640 Challenging Global Waste Management – Bioremediation to Detoxify Asbestos.
641 Frontiers in Environmental Science 8. https://doi.org/10.3389/fenvs.2020.00020
642 Wei, B., Ye, B., Yu, J., Jia, X., Zhang, B., Zhang, X., Lu, R., Dong, T., Yang, L., 2013.
643 Concentrations of asbestos fibers and metals in drinking water caused by natural
644 crocidolite asbestos in the soil from a rural area. Environ Monit Assess 185, 3013–
645 3022. https://doi.org/10.1007/s10661-012-2768-9

WHO - World Health Organization, 2021. Asbestos in drinking water: background document for development of WHO Guidelines for drinking-water quality. World Health Organization.

WHO - World Health Organization, 2000. Air quality guidelines for Europe. World Health Organization. Regional Office for Europe.

WHO - World Health Organization, 1986. Asbestos and other natural mineral fibres. World Health Organization.

Wu, L., Ortiz, C.P., Jerolmack, D.J., 2017. Aggregation of Elongated Colloids in Water. Langmuir 33, 622–629. https://doi.org/10.1021/acs.langmuir.6b03962